
Estimating the State of Epidemics Spreading with Graph Neural Networks

Abhishek Tomy* · Matteo Razzanelli* ·
Francesco Di Lauro · Daniela Rus ·
Cosimo Della Santina

Abstract When an epidemic spreads into a population, it is often unpractical or impossible to have a continuous monitoring of all subjects involved. As an alternative, algorithmic solutions can be used to infer the state of the whole population from a limited amount of measures. We analyze the capability of deep neural networks to solve this challenging task. Our proposed architecture is based on Graph Convolutional Neural Networks. As such it can reason on the effect of the underlying social network structure, which is recognized as the main component in the spreading of an epidemic. We test the proposed architecture with two scenarios modeled on the CoVid-19 pandemic: a generic homogeneous population, and a toy model of Boston metropolitan area.

Keywords Nonlinear Inference, Network Dynamics, State Estimation, Epidemics, CoVid-19

*These authors contributed equally to this work.

Abhishek Tomy
Cognitive Robotics Department, 3ME, TU Delft, Delft, Netherlands.

Matteo Razzanelli
Proxima Robotics srl, Pisa 56124, Italy.

Francesco Di Lauro
Big Data Institute, University of Oxford, Oxford, UK.

Daniela Rus
Computer Science and Artificial Intelligence Laboratory (CSAIL), Massachusetts Institute of Technology (MIT), 32 Vassar St, Cambridge, MA 02139, United States.

Cosimo Della Santina
Cognitive Robotics Department, 3ME, TU Delft, Delft, Netherlands;
Institute of Robotics and Mechatronics, German Aerospace Center (DLR), Oberpfaffenhofen, Germany.
E-mail: cosimodellasantina@gmail.com

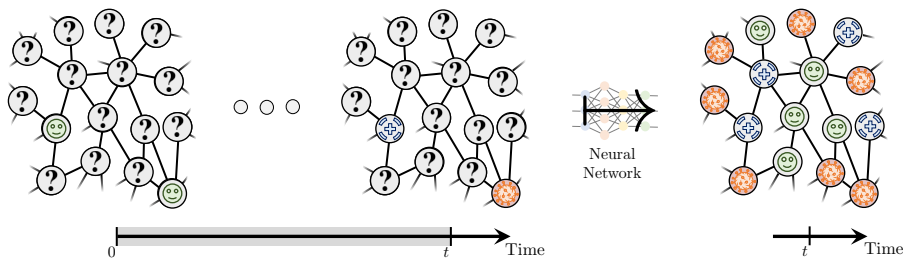


Fig. 1 The goal of this work is to test the use a neural architecture to extract the full state of an epidemic spreading on a social network, from the knowledge of the health state evolution of a small set of subjects.

1 Introduction

Many natural and artificial systems can be described with models whose state assumes value on a graph rather than on a standard Euclidean space. Within this class of systems, the problem of estimating the full state from partial measurements is a very relevant one. If the network follows linear and continuous dynamics, standard techniques can be used. Yet, things get substantially more complicated as soon as non-ideal effects are modeled. For example, (Battistelli et al., 2012) introduces constraints in communications bandwidth. State estimation for networks with distributed delays is discussed in (Liu et al., 2008). A similar problem is dealt in (Wang et al., 2005) for the state estimation of a delayed neural network with known output, and in (Xu et al., 2017) for parameter uncertainty and randomly occurring distributed delays. The case of switched networks with communication constraints is discussed in (Zhang et al., 2017). In this context, much attention has also been devoted to distributed estimation algorithms (Soatti et al., 2016; Ding et al., 2019). For example, (Liu et al., 2017) proposes a consensus-based Kalman filter for sensor networks subjected to random link failures, (Ding et al., 2017) introduces a distributed filter robust to malicious attacks, and (Battistelli and Chisci, 2016) proposes a distributed extended kalman filter for sensor networks measuring a single nonlinear dynamics.

A network dynamics with interesting applications and behavior is the one describing the spreading of an epidemic within a fixed population (Kiss et al., 2017). An effective way of modeling this behavior is to describe the social network as a graph. Each node represents either a subject or a group of subjects, and the arcs the contacts. Simple rules are then used to describe the spreading. For example, these models have been used to describe the spreading of Covid-19. In (Linka et al., 2020) nodes represents European nations. The use of multi-level networks is discussed in (Nande et al., 2021). A survey on the interplay of diseases, behaviors, and information spreading in epidemics is provided in (Wang et al., 2019). Network models have been later extended to simplicial complexes in (Iacopini et al., 2019).

Estimating the state of a epidemics from a reduced number of measurements has clear practical implications. For example, being able to estimate not only the number of infected subjects, but also who those infected subjects are, can allow to implement precise isolation policies (Bahr et al., 2009; Block et al., 2020), feedback strategies (Di Lauro et al., 2020; Kompella et al., 2020), and possibly prevent the generation of clusters (Shim et al., 2020). Nonetheless, we are not aware about previous works in epidemiology dealing with this challenge on the subject (i.e. node) level. Several works deal instead with the much more common problem of extracting robust statistics on the total amount of subjects being infected, recovered, hospitalized etc (Péni et al., 2020; Britton et al., 2019). This estimation can be used to forecast the evolution of the epidemics (Valle, 2020; Tizzoni et al., 2012). Despite requiring to reason on the network dynamics, the task is still such that it can be attacked with model based techniques, since it is essentially a forward integration.

Instead, estimating the full state of the epidemics is an essentially more difficult problem since it requires reasoning backward on the effects that the nodes of which we know the state could have had on the unknown states. This task is made even harder by the highly nonlinear, state-discrete, and stochastic dynamics which characterizes these systems (see Sec. 2). This makes very hard to make inference on the level of the subjects directly using model based techniques. In this work we investigate the use of deep learning for creating a nonlinear inference system which can solve the discussed problem (Brunton and Kutz, 2019). Recently, many works have dealt with the generalization of deep learning to non Euclidean domains (Bronstein et al., 2017). Particular interest have been given to deep learning on graphs (Scarselli et al., 2008; Zhou et al., 2018; Bacciu et al., 2020), i.e. to the learning from data of the graph type. Many of these techniques have been categorized under the umbrella term Graph Neural Networks (GNNs). We are interested here in the use of GNNs as classifiers of nodes. The goal is to determine the labeling of nodes by integrating available information on them and on their neighborhood (Kipf and Welling, 2016). This is for example used as a recommendation engine - see Pinterest (Ying et al., 2018), and Uber Eats (Jain et al., 2019). This task naturally generalizes to the case of state reconstruction, by considering as desired output the full state of the system. We apply this strategy to epidemics, by combining multiple GNN layers with a mechanism for codifying temporal information. The goal of this work is summarized in Fig. 1. We test the results by using state of the art models of epidemics, with particular focus on CoVid-19 spreading in Italy and United States. Our results show that GNNs can be a viable solution to state reconstruction problem, even when the number of monitored subjects is as low as the 5% of the population.

Note that several works already applied GNNs to epidemics, specifically in the CoVid-19 context. Yet the focus has been different w.r.t. the present work. In (Kapoor et al., 2020; Gao et al., 2020) graph neural networks are used to forecast the pandemic evolution. An inverse problem is instead tackled in (Cutura et al., 2020), where authors deal with the temporal reconstruction of

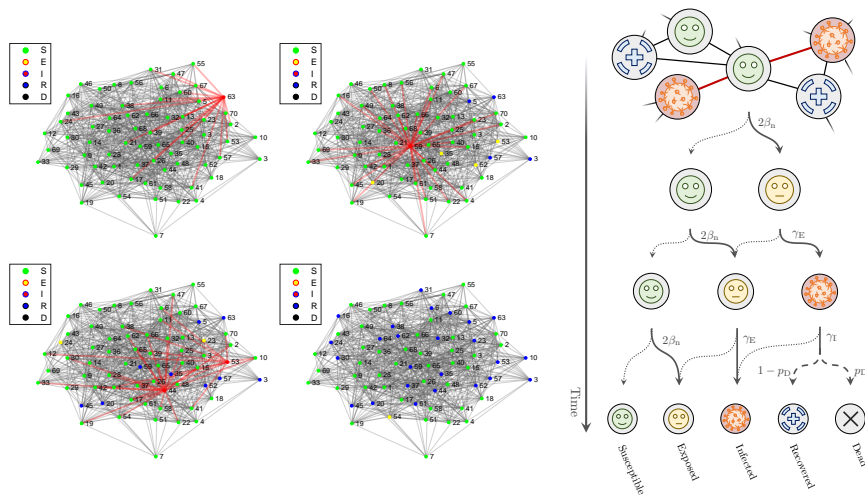


Fig. 2 (left) four snapshots of the state of a small Erdős-Rényi network of size 70 with average degree 20. Links in red carry the infection from an infectious node to a susceptible neighbor. (right). Representation of the transitions a node might undergo with the epidemic model.

the epidemics spreading. Similarly, in (Shah et al., 2020) these techniques are used to identify the patient zero.

2 Epidemics on Networks

Deterministic models for epidemic spreading on a population are well-known because of their simplicity and their usefulness in terms of giving good prediction in terms of aggregate statistics (such as the total number of infected nodes) of the population. Yet, these models do not allow to describe the actual spreading of the epidemics on a population, thus preventing the implementation of targeted measures. For our objective, we need a model that can capture the fact that each individual is part of a social structure, and that the intrinsic hazard of getting infected depends not only on how many people they interact with, but also on how far they are from clusters of infections. A natural candidate is the framework of Network Epidemiology (Pastor-Satorras et al., 2015; Kiss et al., 2017). This framework allows to separate the topological properties of a contact network from the biological dynamics of the disease progression.

2.1 Network Model

A network is described as a set (V, \mathcal{E}) , where V is a set of N nodes (or vertices), and \mathcal{E} is a set of edges (or links) connecting nodes, i.e. tuples $\{u, v\}$, where $u, v \in V$. In terms of modeling, individuals are associated with nodes, and contacts that are at risk of carrying the disease as links between nodes. For sim-

plicity, we consider undirected networks, such that $\{u, v\} \in \mathcal{E} \iff \{v, u\} \in \mathcal{E}$. Figs. 2 shows a pictorial representation of network.

2.2 Epidemic model on Network

We consider a model for disease transmission inspired by recent modeling of Covid-19 Yang et al. (2020); He et al. (2020). Each individual is in one of the following states: S (susceptible), E (exposed), I (infected/infectious), R (recovered), or D (deceased). For this reason, this model is known as SEIRD. Fig. 2 illustrates the possible transitions of a susceptible node that is in contact with two infectious neighbors. Outbreaks are modeled as Markovian processes on the generated network, in which an infected node spreads the disease, via links, to its susceptible neighbors at a constant rate β , turning them into exposed. Exposed nodes represent people who are undergoing their latent period, and are about to become infectious. The next transitions that exposed nodes undergo are network-independent. An E node becomes I after a time exponentially distributed with rate γ_E . Once a node is infectious, he transmits the disease to its neighbors at a constant rate β . The node eventually stops being infectious after an exponentially distributed random time with rate γ_I . When this happens, with probability p_D the node becomes D - representing individuals that do not survive to the disease. The remaining nodes are instead recovered and play no further role in the epidemic. At time $t = 0$, $I(0) = N_I(0) \ll N$ randomly chosen nodes are infected. The remaining ones are initialized as susceptible. We use a Gillespie algorithm (Gillespie, 1977) adapted to networks (Kiss et al., 2017) to simulate this process. In Fig 2 we show a realization of an outbreak on a network of modest size, to highlight how the topology impacts the dynamics.

We describe the the evolution of the state of the pandemic on the network as

$$x : \mathbb{R}^+ \rightarrow \{S, E, I, R, D\}^N. \quad (1)$$

Therefore at each time $t > 0$ the variable $x(t)$ provides a full picture of the spreading of the disease. Without loss of generality, we consider t to be expressed in days. We refer to the state of the node $i \in V$ as $x_i \in \{S, E, I, R, D\}$.

3 State inference from incomplete data

3.1 Goal

Consider the graph (V, \mathcal{E}) describing the social network. We hypothesize to have full knowledge of the state of a subset of nodes $\mathcal{M} \subset V$ at the end of each day. We will populate \mathcal{M} by selecting nodes from V according to a uniform random distribution. We therefore define the set of measurements as $y \in \{S, E, I, R, D\}^{\#\mathcal{M}}$. Finally, for the prediction purposes, classes are

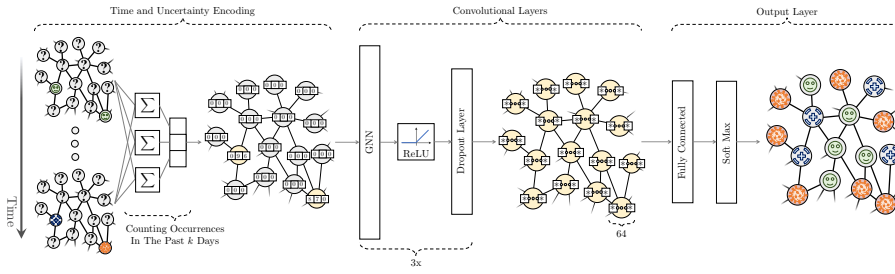


Fig. 3 The proposed architecture is made up of three stages. The first one samples data from the evolution of the known nodes y in the past k days, and counts the occurrences of the three classes. In this way it creates labels l encoding the temporal information. The second stage performs most of the computation, and it is made of three graph convolutional layers. Finally, the high dimensional internal information is compressed again by the output layer, i.e. a fully connected network and a soft max. The output is an estimation of the current full state of the epidemics spreading.

combined based on their usefulness in intervention into 3 classes. Our goal is thus to find an algorithm which implements the following mapping

$$\{V, \mathcal{M}, \mathcal{E}, y([0, t])\} \mapsto \tilde{x}(t) \quad (2)$$

where $\tilde{x} \in \{S, E+I, R+D\}^N$ is our reconstructed state, with $E+I$ representing nodes that either exposed or infected, and with $R+D$ We want (2) to be such that \tilde{x} is as coherent as possible with the full state x . Indeed, in the practice we are only interested in knowing if the subject is healthy (S), has contracted the virus (E and I), or is no more infected (R and D). This challenge is summarize in Fig. 1.

Note that in this work we assume full knowledge of the social structure (V, \mathcal{E}) as input for the network. This is a strong assumption that we will relax in future work. Also, we will discuss the robustness of the algorithm to changes of topology.

3.2 First stages

We start by transforming $y([0, t])$ in a data structure that can be effectively put as input of our neural network. More specifically, we introduce the nodes label $l \in \mathbb{N}^N \times 3$. For all $i \in \mathcal{M}$, the vector l_i codifies the state of the nodes in the past k days. We do that in a bag-of-words fashion (Weinberger et al., 2009). We sample y on a daily basis $y_i([t]), y_i([t] - 1) \dots, y_i([t] - k + 1)$. The value $k \in \mathbb{N}$ is an hyperparameter which will be later optimized. We then take $l_{i,1}$ equal to the number of times the state S appears in the sampling. Similarly, $l_{i,2}$ counts the occurrences of E and I , and $l_{i,3}$ of R and D . Therefore the sum of elements in l_i is always equal to k for $i \in \mathcal{M}$. The remaining nodes are labeled as *unknown* by taking $l_i = 0$ for all $i \notin \mathcal{M}$. These operations are graphically summarized in the left part of Fig. 3.

3.3 Neural architecture

Graph Neural Networks operate in the domain of the graph. In the graph, each node comes with its label. A common framework in the GNN is the classification problem setup where the goal is to predict the label of the unlabeled nodes given the labeled ones. As mentioned before we want to predict the full state of the pandemics spreading x , see Fig. 1.

The central part of Fig. 3 shows the core GNN layers in our architecture. The target of our GNN is to learn the state embedding $l_i \in \mathbb{N}^3$ for $i = 1, 2, 3$, which contains the information of neighborhood for each node. The initial node feature corresponds to the node state itself, encoded in binary vector $\in \mathbb{N}^3$ that contains only one element equal to 1. We preprocess this information by integrating l_i along the time horizon of k . We cannot use k too big to avoid that the neural network leverages on this pattern to recognize that the state coincide with the node label. Due to the fact that it is a classification problem setup, we then mask a certain percentage of node (95 – 90 – 80%) depending on the scenario we are considering. We finalize the preprocess by loading data by batch by using the Dataloader class defined inside the Pytorch library (Paszke et al., 2019). Thanks to a specific variable, named 'batch', the data loader can associates node and edges to a specific graph. Since a DataLoader aggregates nodes, edges and the features from different graphs into batches during the message passing layers, the GNN model needs this information to know which nodes belong to the same graph. For what concern message passing layer, it describes how l_i is passed through the layers of the network to create the node embedding. As we know, the message passing layer is the result of the generalization of the convolution operator by extending the concept of the neighbourhood from pixels to nodes (Kipf and Welling, 2016). Given the state of the node i at the layer h , l_i^h we find the l_i^{h+1} by applying the activation function of the message passing layer to l_i^h and the aggregation of l_j^h where $j \in \mathcal{N}_i$ is a neighbour of node i (and \mathcal{N}_i is the neighbourhood of node i). As the node embedding evolve through the message passing layers, as the knowledge of the neighborhood of each single node increases. Thus, the message passing layers enlarge, in general, the size of the node feature. The number of the message passing layers could be considered again as a hyperparameter. Without loss of generality, in our case, three message passing layers with a rectifier as the activation function (ReLU) are considered. The first message passing layer has an input size of 3 (i.e. the number of features), and output size of 64. The second and the third message passing layers have an input and output sizes of dimension 64. Between layers there the dropout regularization method is used during training to avoid over-fitting.

As a result of this processing, each node is equipped with a rich description of its possible state as inferenced by its neighbours own representations. This state need to be converted into one of the three states $\{S, E + I, R + D\}$. This is done through the Output Layer (right part of Fig. 3). First we have a fully connected layer. Its input size is 64 and output size of 3. It is defined with a linear activation function. Then, a *softmax* function is introduced as defined

in the Pytorch library. It is applied to the observation l_i so to retrieve the highest probability that the node will be labeled with a certain class.

For what concerns the training, an Adam optimizer with a fixed learning rate is defined and we select loss $L_1(\cdot)$ as the cross entropy. Given the unbalanced classes $c \in \{S, E + I, R + D\}$ we compute weight w_c to normalize observation l_i . The weight of each class is determined by the $\frac{N_{\max}}{N_c}$ where N_{\max} is the the number of observations in the class with maximum occurrence and N_c is the number of observations or nodes belonging to class c in the training set. We use the loss function for measuring the performance of the algorithm as described by the Pytorch library. The losses are then averaged across observations:

$$L_1(\cdot) = \frac{\sum_{c=1}^3 \text{loss}(x_c)}{\sum_{c=1}^3 w_c}. \quad (3)$$

Given a fixed number of epochs (250 in our case) we train our network and we measure the loss function as previously defined to measure the loss. Hyperparameter optimization is done using balanced accuracy. Balanced accuracy is calculated as the average of the proportion corrects of each class individually. Balanced accuracy is suitable for datasets with class imbalance unlike other metrics which may favour results from the majority class.

4 Simulations

We test the proposed architecture in two scenarios, with different topological characteristics. The first one is an homogeneous network, in which any node has the same probability of being connected with all the others. We use this scenario to test extensively the effectiveness and scalability of the method. The second scenario is instrumental to test the neural architecture in a more challenging setting, closer to a real world scenario.

4.1 Scenario 1: random network

We consider Erdős-Rényi networks, which are a class of well-known network models. Such random networks are relatively simple to describe, and at the same time offer some heterogeneity in terms of the degree distribution. The generative algorithm can be described as follows: we start with N isolated nodes, then we place a link between any two nodes with probability $0 < p < 1$. The degree distribution of the network is therefore binomial $\mathbb{B}(N, p)$. We showcase results for networks with average degree $\langle k \rangle = 30$. This value is comparable with the number of daily contacts at risk as measured in a recent survey (Melegaro et al., 2011).

We generate training set from 80 realizations, each one happening on a different and randomly generate social network with a population of 500 nodes. The epidemic spreads between 0 and 120 days. Yet in the initial month, the behavior is quite stationary due to the well-know slow increase of the total

Table 1 Accuracy (Ac.) and precision (Pr.) of the classification for Scenario 1, evaluated only on the nodes which are not in \mathcal{M} . The testing set is generated with networks of 500 nodes. Three levels of supervision are considered - i.e., number of nodes of V which are in \mathcal{M} as well.

	Ac., 5%	Pr., 5%	Ac., 10%	Pr., 10%	Ac., 20%	Pr., 20%
S	0.93	0.84	0.93	0.84	0.93	0.85
$E+I$	0.52	0.56	0.51	0.57	0.51	0.57
$R+D$	0.74	0.78	0.75	0.77	0.76	0.77
All	0.75	-	0.75	-	0.76	-

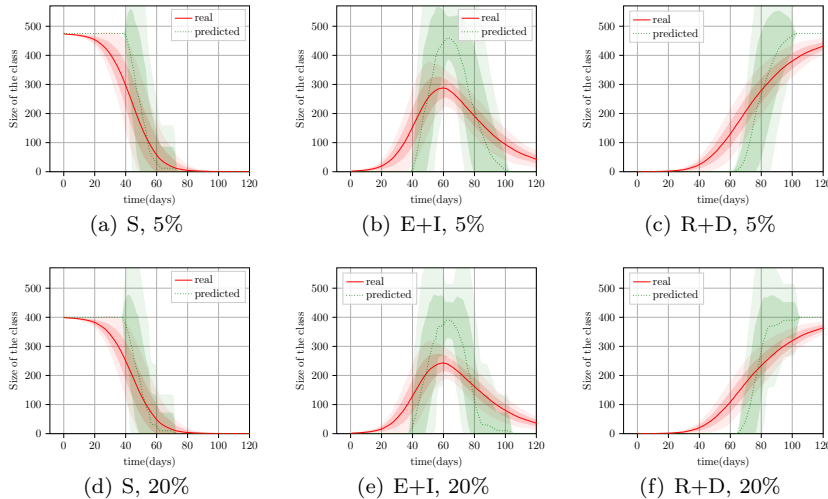


Fig. 4 Evolution of overall statistics associated to the epidemics, when evolving on a medium-small homogeneous network (scenario 1). More specifically, we show the amount of nodes which are susceptible - Panels (a,d) - which got infected by the pathogen - Panels (b,e) - and which either recovered or died - Panels (c,f). Actual evolutions are in red, while estimations are in green. The solid lines represent the mean, while the translucent areas the variance. Training and testing sets are made of realizations produced by simulating the epidemic spreading on random social networks of 500 subjects. In Panels (a-c) only 5% of subjects is tested at any time, while in Panels (d-f) this number reaches 20%.

number of infected subjects. Therefore, a few samples from the initial days is enough to learn the pattern during that period. Only 3 random days are selected from the first month of each realization. All the remaining days from 30 to 120 are used for training. The hyperparameters are 0.3 for dropout, 64 hidden units, 3 layers. We use a learning rate of 0.0002, we train for 250 epochs, with a batch size of 256.

At first, we test the trained architecture on a set of 40 realizations, representing evolutions on randomly generated social networks with 500 nodes (same size of the training set). We repeat the analysis for the cases in which the size of \mathcal{M} (i.e. monitored subjects) is 5%, 10%, 20% of the size of V (i.e. the total amount of subjects in the considered population). It is worth to no-

Table 2 Accuracy (Ac.) and precision (Pr.) of the classification for Scenario 1, evaluated only on the nodes which are not in \mathcal{M} . The testing set is generated with networks of 10^5 nodes. Three levels of supervision are considered - i.e., number of nodes of V which are in \mathcal{M} as well.

	Ac., 5%	Pr., 5%	Ac., 10%	Pr., 10%	Ac., 20%	Pr., 20%
S	0.97	0.92	0.96	0.92	0.93	0.85
$E+I$	0.50	0.58	0.50	0.57	0.51	0.57
$R+D$	0.79	0.81	0.80	0.81	0.76	0.77
All	0.83	-	0.83	-	0.83	-

tice that this is a very sparse amount of information. Indeed, 10% of tests with an average connectivity of 10 means that any node has on average just a single neighbor whose state is known (see Fig. 1 to get a visual sense of this ratio). Accuracy and precision of the predictions are provide in Tab. 4.1. Note that these values are evaluated only on the nodes which are not part of \mathcal{M} since they are always perfectly known. Thus, we prefer to leave them out to not artificially increase the performance of the neural network. Interestingly, the quality of the predictions do not change significantly with the size of \mathcal{M} . In general classes with larger amount of subjects have better performance. This can be due to the higher amount of examples which are available from the training set. Overall the performance is satisfactory, with a general accuracy always higher than 0.75. To get a sense of how these results reflect in the estimation of cumulative statistics of the pandemic evolution, in Fig. 4 we plot the total size of each class against the amount of nodes which are classified to be part of that class. The match is good. The network is not sensitive to small deviations of S and $R+D$ from the maximum and the minimum value. This may be due to the fact that so small variations may not be captured by changes in \mathcal{M} . Also, the neural network tends to over estimate the presence of subjects which got infected at the pick. It is very important to stress here that these overall statistics serve here only to get a sense of the overall quality of the network predictions. The goal of the neural architecture is indeed not to estimate these values directly, but the exact way in which each class is spread over the social network. This is an important distinction because the direct estimations of the size of the three classes is a relatively simple task, as discussed in the Introduction.

A nice property that our architecture inherits from Graph Convolutional Neural network is that once trained it can be applied to graphs of any size. This is because we directly learn the weights of the convolution operator, which can then be applied to notworks of all sizes. There is however no guarantee that the classification will keep being effective. Indeed, the way in which the pandemic evolves is clearly affected by the size of the social network despite the local rules remaining the same. We therefore tested the ability of the architecture to generalize to larger populations by building an additional testing set of 10 realizations with a total number of nodes which is several orders of magnitude larger than before: 10^5 subjects. It is very important to stress that no re-

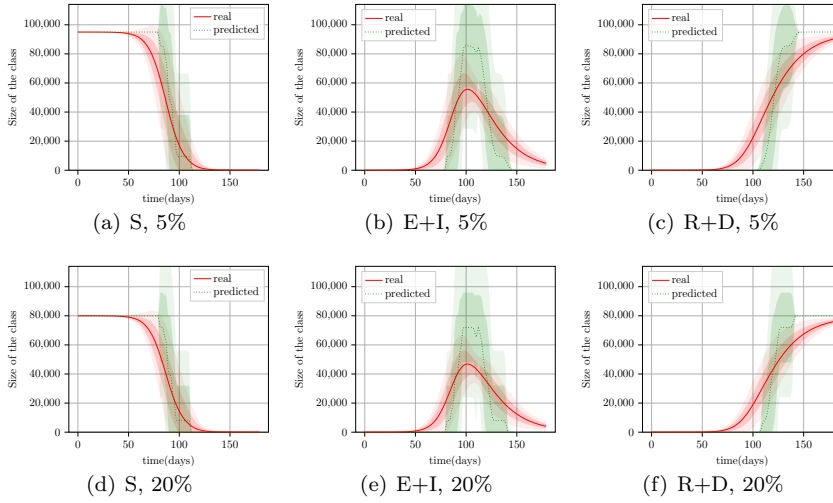


Fig. 5 Evolution of overall statistics associated to the epidemics, when evolving on an homogeneous network (scenario 1). Actual evolutions are in red, and estimations in green. The solid lines represent the mean, while the translucent areas the variance. The testing set is made of realizations produced by random social networks of 10^5 subjects. Instead the training set contains only networks which are 500 nodes big. In Panels (a-c) only 5% of subjects is tested at any time, while in Panels (d-f) this number reaches 20%.

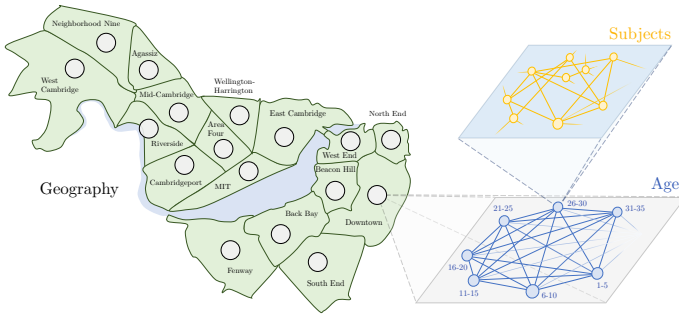


Fig. 6 The second scenario is a toy model inspired by the spreading of CoVid in the Boston and Cambridge, Massachusetts. The topology of the graph is built on three layers, which integrate the geographical distribution of the population, the demographics, and the subject level variability.

training is performed. Therefore, we are training the neural architecture with a small-village community, and testing it with a medium size city. Tab. 4.1 and Fig. 5 show the result of this analysis. No essential differences can be observed. Overall the performance is still satisfactory, with a general accuracy which is even higher than the previous test set and always equal to 0.83. This may be due to the fact that larger social networks generate more homogeneous distributions of the illness since the border-effects are less dominant.

4.2 Scenario 2: Boston

The second scenario we consider aims at modeling a more realistic social structure, such as the one of a relatively big city. We need to consider both a model that takes into account the existence of different neighborhoods and the age distribution of people living in that area. We take as a reference the City of Boston and Cambridge, Massachusetts, USA.

The generative model, which takes inspiration from the work in (Mistry et al., 2021), is divided into three steps, as in fig. 6. Initially, we outline a map of the neighborhoods of the urban area we focus on. At this stage, each neighborhood is a network on its own. The size of each neighborhood is taken from the official website of the city of Boston¹ and Cambridge². Within each neighborhood, the topology reflects the contact patterns between different age-classes, as described in the Supplementary material of (Mistry et al., 2021). To do so, we cohort the population into age groups of size 5 years, and we model the contact patterns among groups based on their age with a stochastic block model (Holland et al., 1983). Stochastic block models are generative models for random graphs that are used to generate topologies that have a community-like structure. Each node is given a unique label (the age cohort). Then, we define a symmetric matrix (known as Affinity matrix) whose elements are $\mathcal{A}_{ij} = p_{ij}$, where p_{ij} is the probability that a node whose label is i is in contact with a node whose label is j . The Affinity matrix we use is the Massachusetts age-contact matrix, as described in the supplementary material of (Mistry et al., 2021). The last step is to connect different neighborhoods by allowing nodes in each neighborhood to have links with nodes from other neighborhoods. To do so, we consider a diffusion-like procedure: for each couple of neighborhoods we place a random number of links between randomly selected nodes from both communities, depending on the length of the shortest path connecting the two on the geographical level: neighborhoods at distance d from each other will share, on average, $1/d$ links with respect to neighborhoods at distance 1. The number of links shared between any two communities is drawn from a Binomial with probability $p = \frac{1}{50} \frac{1}{d}$.

We generated a training composed of 20 realizations, each one happening on a different and randomly generated social network with a population of 10^4 nodes. This is one order of magnitude less than the actual population of that area. This choice has been imposed by limits on the hardware resources available. In this scenario, the epidemic spreads over a relatively long period of time, with each day being of importance and different. Hence we select a total of 201 days from each realization, starting 100 days before the pick of the infection, and ending 100 days after. No sample is removed. The hyperparameters are 0.4 for dropout, 64 hidden units, 3 layers. We use a learning rate of 0.0002, we train for 250 epochs, with a batch size of 64.

¹ <http://www.bostonplans.org/getattachment/7987d9b4-193b-4749-8594-e41f1ae27719>

² https://www.cambridgema.gov/-/media/Files/CDD/FactsandMaps/profiles/demo_profile_neighborhood_2019.pdf

Table 3 Accuracy (Ac.) and precision (Pr.) of the classification for Scenario 2 (Boston), evaluated only on the nodes which are not in \mathcal{M} . Three levels of supervision are considered - i.e., number of nodes of V which are in \mathcal{M} as well.

	Ac., 5%	Pr., 5%	Ac., 10%	Pr., 10%	Ac., 20%	Pr., 20%
S	0.67	0.97	0.67	0.98	0.67	0.98
$E+I$	0.75	0.14	0.78	0.14	0.80	0.15
$R+D$	0.78	0.79	0.79	0.79	0.80	0.80
All	0.72	-	0.72	-	0.73	-

We test the effectiveness of the proposed approach by collecting a testing set made of 10 realizations. Each realization is an evolution of the epidemic on a different and randomly generated social network (following the same statistical characteristics of the testing set). As for scenario 1, also here we test the case of size of \mathcal{M} (i.e. tested subjects) being 5%, 10%, or 20% of the total population. Results are shown in Tab. 4.2 and Fig. 7. Although lower in the easier scenario 1, the accuracy is consistently good across classes and conditions. Yet, the accuracy of S is a bit lower than before, and the precision of $E + I$ is very low. This is because the neural architecture tends to wrongly label a number of nodes which are susceptible as infected. Yet, it is important to underline here that the neural network is working with a quite small amount of information on the spreading of infected subjects. Indeed, at its pick $E + I$ is less than the 10% of the population, which with 10% of measures means that the algorithm can rely on the knowledge of 10^2 infected nodes. This behavior is also evident in Fig. 7, where the total number of susceptible subjects is higher than estimated, and vice versa the infected subjects are lower than the neural network thinks. It is again important to stress that the proposed algorithm is optimized to estimate the distribution of subjects rather than the total size of each class, which should therefore be regarded as a secondary index. It is also interesting that the algorithm rarely does the opposite error, i.e. classifying S as $E + I$. The precision of S is indeed above 97%. Although not explicitly forced in training phase, this behavior makes very much sense in the practice since it is better to isolate healthy subjects than not to act on infected ones.

5 Discussion and Conclusions

With this work we investigated the use of Graph Neural Networks to develop state observers for epidemics evolving on social networks. The results are promising. The neural architecture can approximate the overall state with an accuracy which is always above the 70%, even when the sample space is as small as 5% of the total population.

Nonetheless, there are several directions towards which our results may be improved which we aim at investigating in the future. First, future work will be devoted to adding explicit dynamic reasoning within the neural network, for example by introducing recurrent layers (Liang et al., 2016). This

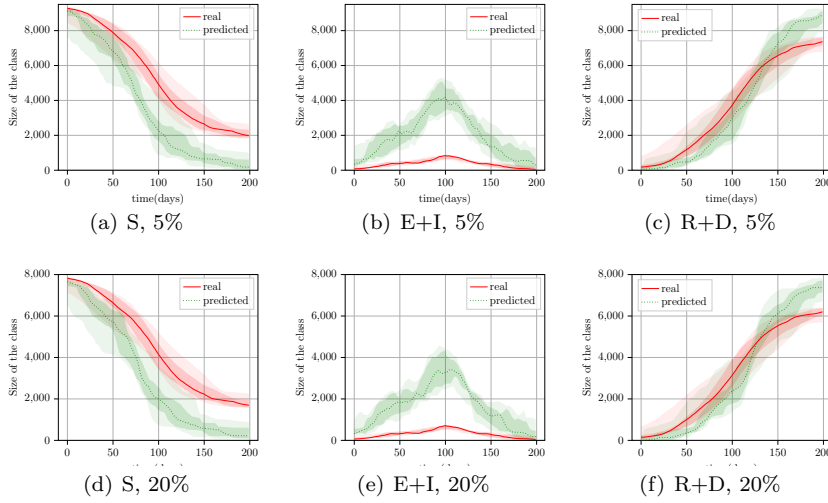


Fig. 7 Evolution of overall statistics associated to the epidemics, when evolving on a toy model inspired by the Boston and Cambridge (MA,USA) areas. We show the amount of number of susceptibles in Panels (a,d), the infected and exposed in Panels (b,e), the recovered or dead in Panels (c,f). Actual evolutions are in red, while estimations are in green. The solid lines represent the mean, while the translucent areas the variance. Training and testing sets are made of realizations produced by simulating the epidemic spreading on random social networks of 500 subjects. In Panels (a-c) only 5% of subjects is tested at any time, while in Panels (d-f) this number reaches 20%.

should help boost the capability of the neural network of discerning between exposed and infected, and between infected and recovered (or dead). Indeed, these transitions are essentially time dependent and can be extracted from associating an internal dynamics to the initial recognition that a node entered in the exposed state. Yet, it is worth mentioning that stacking LSTMs layers in between the GNNs did not produce a statistically relevant increasing of the network performance and as such has not been included in the present work. Similarly the use of attention mechanisms (Veličković et al., 2017) have been tested but not included due to the negligible increment of performance that they resulted into. Finally, we believe that a very important assumption to be relaxed is the full knowledge of the social network (see Sec. 3.1). Several algorithms are being proposed that can extract the social structure from GPS localization and other mobility information provided by contact tracing apps (Ferretti et al., 2020; Cheng et al., 2020). Data driven methods can then possibly be used to infer the graph topology itself (Segarra et al., 2017; Giannakis et al., 2018).

Conflicts of Interest

The authors declare that they have no conflict of interest.

Funding

This work is supported by the TU Delft CoVid-19 response fund, and by the Leverhulme Trust through the Research Project (Grant number RPG2017-370).

References

- Bacciu D, Errica F, Micheli A, Podda M (2020) A gentle introduction to deep learning for graphs. *Neural Networks*
- Bahr DB, Browning RC, Wyatt HR, Hill JO (2009) Exploiting social networks to mitigate the obesity epidemic. *Obesity* 17(4):723–728
- Battistelli G, Chisci L (2016) Stability of consensus extended kalman filter for distributed state estimation. *Automatica* 68:169–178
- Battistelli G, Benavoli A, Chisci L (2012) Data-driven communication for state estimation with sensor networks. *Automatica* 48(5):926–935
- Block P, Hoffman M, Raabe IJ, Dowd JB, Rahal C, Kashyap R, Mills MC (2020) Social network-based distancing strategies to flatten the covid-19 curve in a post-lockdown world. *Nature Human Behaviour* 4(6):588–596
- Britton T, Pardoux E, Ball F, Laredo C, Sirl D, Tran VC (2019) Stochastic epidemic models with inference. Springer
- Bronstein MM, Bruna J, LeCun Y, Szlam A, Vandergheynst P (2017) Geometric deep learning: going beyond euclidean data. *IEEE Signal Processing Magazine* 34(4):18–42
- Brunton SL, Kutz JN (2019) Data-driven science and engineering: Machine learning, dynamical systems, and control. Cambridge University Press
- Cheng HY, Jian SW, Liu DP, Ng TC, Huang WT, Lin HH, et al. (2020) Contact tracing assessment of covid-19 transmission dynamics in taiwan and risk at different exposure periods before and after symptom onset. *JAMA internal medicine* 180(9):1156–1163
- Cutura G, Li B, Swami A, Segarra S (2020) Deep demixing: Reconstructing the evolution of epidemics using graph neural networks. arXiv preprint arXiv:201109583
- Di Lauro F, Kiss IZ, Rus D, Della Santina C (2020) Covid-19 and flattening the curve: A feedback control perspective. *IEEE Control Systems Letters* 5(4):1435–1440
- Ding D, Wang Z, Ho DW, Wei G (2017) Distributed recursive filtering for stochastic systems under uniform quantizations and deception attacks through sensor networks. *Automatica* 78:231–240
- Ding D, Han QL, Wang Z, Ge X (2019) A survey on model-based distributed control and filtering for industrial cyber-physical systems. *IEEE Transactions on Industrial Informatics* 15(5):2483–2499
- Ferretti L, Wymant C, Kendall M, Zhao L, Nurtay A, Abeler-Dörner L, Parker M, Bonsall D, Fraser C (2020) Quantifying sars-cov-2 transmission suggests epidemic control with digital contact tracing. *Science* 368(6491)

- Gao J, Sharma R, Qian C, Glass LM, Spaeder J, Romberg J, Sun J, Xiao C (2020) Stan: Spatio-temporal attention network for pandemic prediction using real world evidence. arXiv preprint arXiv:200804215
- Giannakis GB, Shen Y, Karanikolas GV (2018) Topology identification and learning over graphs: Accounting for nonlinearities and dynamics. *Proceedings of the IEEE* 106(5):787–807
- Gillespie DT (1977) Exact stochastic simulation of coupled chemical reactions. *The Journal of Physical Chemistry* 81(25):2340–2361, DOI 10.1021/j100540a008
- He S, Peng Y, Sun K (2020) Seir modeling of the covid-19 and its dynamics. *Nonlinear Dynamics* 101(3):1667–1680
- Holland PW, Laskey KB, Leinhardt S (1983) Stochastic blockmodels: First steps. *Social Networks* 5(2):109–137, DOI [https://doi.org/10.1016/0378-8733\(83\)90021-7](https://doi.org/10.1016/0378-8733(83)90021-7)
- Iacopini I, Petri G, Barrat A, Latora V (2019) Simplicial models of social contagion. *Nature communications* 10(1):1–9
- Jain A, Liu I, Sarda A, Molino P (2019) Food discovery with uber eats: Using graph learning to power recommendations
- Kapoor A, Ben X, Liu L, Perozzi B, Barnes M, Blais M, O’Banion S (2020) Examining covid-19 forecasting using spatio-temporal graph neural networks. arXiv preprint arXiv:200703113
- Kipf TN, Welling M (2016) Semi-supervised classification with graph convolutional networks. arXiv preprint arXiv:160902907
- Kiss IZ, Miller JC, Simon PL, et al. (2017) *Mathematics of epidemics on networks*
- Kompella V, Capobianco R, Jong S, Browne J, Fox S, Meyers L, Wurman P, Stone P (2020) Reinforcement learning for optimization of covid-19 mitigation policies. arXiv preprint arXiv:201010560
- Liang X, Shen X, Feng J, Lin L, Yan S (2016) Semantic object parsing with graph lstm. In: *European Conference on Computer Vision*, Springer, pp 125–143
- Linka K, Peirlinck M, Sahli Costabal F, Kuhl E (2020) Outbreak dynamics of covid-19 in europe and the effect of travel restrictions. *Computer Methods in Biomechanics and Biomedical Engineering* 23(11):710–717
- Liu Q, Wang Z, He X, Zhou D (2017) On kalman-consensus filtering with random link failures over sensor networks. *IEEE Transactions on Automatic Control* 63(8):2701–2708
- Liu Y, Wang Z, Liang J, Liu X (2008) Synchronization and state estimation for discrete-time complex networks with distributed delays. *IEEE Transactions on Systems, Man, and Cybernetics, Part B (Cybernetics)* 38(5):1314–1325
- Melegaro A, et al. (2011) What types of contacts are important for the spread of infections? using contact survey data to explore european mixing patterns. *Epidemics* 3(3):143 – 151, DOI <https://doi.org/10.1016/j.epidem.2011.04.001>
- Mistry D, Litvinova M, y Piontti AP, Chinazzi M, Fumanelli L, Gomes MF, Haque SA, Liu QH, Mu K, Xiong X, et al. (2021) Inferring high-

- resolution human mixing patterns for disease modeling. *Nature communications* 12(1):1–12
- Nande A, Adlam B, Sheen J, Levy MZ, Hill AL (2021) Dynamics of covid-19 under social distancing measures are driven by transmission network structure. *PLOS Computational Biology* 17(2):e1008684
- Pastor-Satorras R, Castellano C, Van Mieghem P, Vespignani A (2015) Epidemic processes in complex networks. *Reviews of Modern Physics* 87(3):925, DOI 10.1103/RevModPhys.87.925
- Paszke A, Gross S, Massa F, Lerer A, Bradbury J, Chanan G, Killeen T, Lin Z, Gimelshein N, Antiga L, et al. (2019) Pytorch: An imperative style, high-performance deep learning library. *arXiv preprint arXiv:1912.01703*
- Péni T, Csutak B, Szederkényi G, Röst G (2020) Nonlinear model predictive control with logic constraints for covid-19 management. *Nonlinear Dynamics* 102(4):1965–1986
- Scarselli F, Gori M, Tsoi AC, Hagenbuchner M, Monfardini G (2008) The graph neural network model. *IEEE transactions on neural networks* 20(1):61–80
- Segarra S, Marques AG, Mateos G, Ribeiro A (2017) Network topology inference from spectral templates. *IEEE Transactions on Signal and Information Processing over Networks* 3(3):467–483
- Shah C, Dehmamy N, Perra N, Chinazzi M, Barabási AL, Vespignani A, Yu R (2020) Finding patient zero: Learning contagion source with graph neural networks. *arXiv preprint arXiv:2006.11913*
- Shim E, Tariq A, Choi W, Lee Y, Chowell G (2020) Transmission potential and severity of covid-19 in south korea. *International Journal of Infectious Diseases* 93:339–344
- Soatti G, Nicoli M, Savazzi S, Spagnolini U (2016) Consensus-based algorithms for distributed network-state estimation and localization. *IEEE Transactions on Signal and Information Processing over Networks* 3(2):430–444
- Tizzoni M, Bajardi P, Poletto C, Ramasco JJ, Balcan D, Gonçalves B, Perra N, Colizza V, Vespignani A (2012) Real-time numerical forecast of global epidemic spreading: case study of 2009 a/h1n1pdm. *BMC medicine* 10(1):1–31
- Valle JAM (2020) Predicting the number of total covid-19 cases and deaths in brazil by the gompertz model. *Nonlinear Dynamics* 102(4):2951–2957
- Veličković P, Cucurull G, Casanova A, Romero A, Lio P, Bengio Y (2017) Graph attention networks. *arXiv preprint arXiv:1710.10903*
- Wang W, Liu QH, Liang J, Hu Y, Zhou T (2019) Coevolution spreading in complex networks. *Physics Reports* 820:1–51
- Wang Z, Ho DW, Liu X (2005) State estimation for delayed neural networks. *IEEE Transactions on Neural Networks* 16(1):279–284
- Weinberger K, Dasgupta A, Langford J, Smola A, Attenberg J (2009) Feature hashing for large scale multitask learning. In: *Proceedings of the 26th annual international conference on machine learning*, pp 1113–1120
- Xu Y, Lu R, Shi P, Tao J, Xie S (2017) Robust estimation for neural networks with randomly occurring distributed delays and markovian jump coupling.

-
- IEEE Transactions on Neural Networks and Learning Systems 29(4):845–855
- Yang Z, Zeng Z, Wang K, Wong SS, Liang W, Zanin M, Liu P, Cao X, Gao Z, Mai Z, et al. (2020) Modified seir and ai prediction of the epidemics trend of covid-19 in china under public health interventions. *Journal of thoracic disease* 12(3):165
- Ying R, He R, Chen K, Eksombatchai P, Hamilton WL, Leskovec J (2018) Graph convolutional neural networks for web-scale recommender systems. In: *Proceedings of the 24th ACM SIGKDD International Conference on Knowledge Discovery & Data Mining*, pp 974–983
- Zhang D, Wang QG, Srinivasan D, Li H, Yu L (2017) Asynchronous state estimation for discrete-time switched complex networks with communication constraints. *IEEE transactions on neural networks and learning systems* 29(5):1732–1746
- Zhou J, Cui G, Zhang Z, Yang C, Liu Z, Wang L, Li C, Sun M (2018) Graph neural networks: A review of methods and applications. *arXiv preprint arXiv:181208434*